Letter

Characterizing topological excitations of a long-range Heisenberg model with trapped ions

Stefan Birnkammer,[1,2,*] Annabelle Bohrdt,[1,2] Fabian Grusdt,[3,1,2] and Michael Knap[1,2]

[1]*Department of Physics, Technical University of Munich, 85748 Garching, Germany*

[2]*Munich Center for Quantum Science and Technology (MCQST), Schellingstraße 4, München 80799, Germany*

[3]*Department of Physics and Arnold Sommerfeld Center for Theoretical Physics (ASC), Ludwig-Maximilians-Universität München, Theresienstraße 37, München D-80333, Germany*

(Received 12 January 2021; revised 29 March 2022; accepted 17 May 2022; published 3 June 2022)

Realizing and characterizing interacting topological phases in synthetic quantum systems is a formidable challenge. Here, we propose a Floquet protocol to realize the antiferromagnetic Heisenberg model with power-law decaying interactions. Based on analytical and numerical arguments, we show that this model features a quantum phase transition from a liquid to a valence bond solid that spontaneously breaks lattice translational symmetry and is reminiscent of the Majumdar-Ghosh state. The different phases can be probed dynamically by measuring the evolution of a fully dimerized state. We moreover introduce an interferometric protocol to characterize the topological excitations and the bulk topological invariants of the interacting many-body system.

DOI: 10.1103/PhysRevB.105.L241103

Introduction. Recent progress in realizing synthetic quantum systems has offered new opportunities for the experimental characterization and control of topological quantum phases. Topologically nontrivial band structures have been created by periodic driving [1–5], interaction-induced chiral propagation of excitations have been studied in the few-body limit of quantum Hall states [6,7], symmetry protected topological (SPT) phases have been realized [8–11], and quantum spin liquids have been explored with quantum devices [12,13]. While first steps have been taken in realizing interacting topological phases, several challenges remain, in particular concerning the characterization and control of individual topological excitations.

Here, we propose the realization of a dimerized valence bond solid with topologically nontrivial excitations in a Heisenberg model with power-law interactions using trapped ions [14]. This phase arises due to frustration from long-range interactions and is adiabatically connected to the symmetry-broken Majumdar-Ghosh phase [15–17]. When locally deforming this Hamiltonian to introduce bond alternating couplings, it realizes a Haldane SPT phase [18]. Our model therefore illustrates the interplay between spontaneous symmetry breaking and toplogical order. To realize the long-range Heisenberg model in a trapped-ion setting, we propose a Floquet protocol that consists of periodic globally applied $\pi/2$ pulses around different axes of the Bloch sphere; see Figs. 1(a) and 1(b). We determine the phase diagram and propose an interferometric protocol to characterize the topological excitations and the bulk topological invariants of our interacting many-body system.

Model. We investigate a long-range spin-1/2 Heisenberg chain with open boundaries

$$H_{\mathrm{LR}}(\alpha) = \sum_{i<j} \frac{J}{|i-j|^{\alpha}} \left[\hat{S}_i^x \hat{S}_j^x + \hat{S}_i^y \hat{S}_j^y + \hat{S}_i^z \hat{S}_j^z\right], \quad (1)$$

where α is the power-law exponent of the long-range interactions and $J > 0$ is their typical energy scale (for a spin-1 variant of the model see Ref. [19]). When considering only nearest and next-to-nearest neighbor couplings, $H_{\mathrm{LR}}(\alpha)$ reduces to the Majumdar-Ghosh (MG) model [15,16], which exhibits a phase transition from a liquid to a dimerized valence bond solid that breaks the translational invariance of the lattice [17].

The long-range Heisenberg model H_{LR} reduces for $\alpha \to \infty$ to the conventional Heisenberg model with nearest-neighbor couplings, whose ground state is a gapless spin liquid with power-law decaying antiferromagnetic correlations [20]. For the opposite limit of $\alpha \to 0$, each spin interacts equally with all the others and the ground states correspond to arbitrary singlet pairings (see Supplemental Material [21] and Refs. [22–24] therein). For small but finite α, it is energetically favorable to form singlets on neighboring sites as in the Majumdar-Ghosh state

$$|\mathrm{MG}\rangle = \prod_{i}^{L/2} (|\uparrow\rangle_{2i}|\downarrow\rangle_{2i+1} - |\downarrow\rangle_{2i}|\uparrow\rangle_{2i+1})/\sqrt{2}. \quad (2)$$

As a consequence, the ground state breaks translational symmetry. Due to the different behavior of the ground states in the two limits, at least one quantum phase transition occurs at some critical α_c.

To quantitatively determine the phase diagram, we perform density-matrix renormalization group (DMRG) simulations [25,26] and compute the dimerization order parameter

$$d_i = \vec{S}_{2i} \cdot (\vec{S}_{2i+1} - \vec{S}_{2i-1}) \quad (3)$$

as a function of α and for different system sizes L; see Fig. 1(c). The data for the thermodynamic limit was extrapolated from finite-size results by a scaling ansatz $|\alpha - \alpha_c|^{\nu}$. Expressions without spatial indices, indicate in the following averages over the bulk. In our numerical studies, we represent the Hamiltonian as a matrix product operator, in which we

*stefan.birnkammer@tum.de

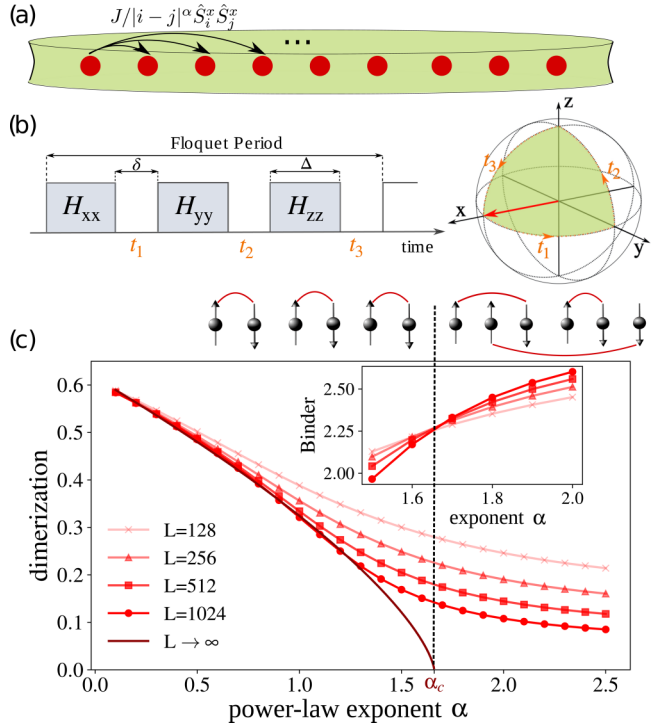

FIG. 1. Floquet protocol and phase diagram. (a) Interactions between ions in a linear Paul trap are of Ising type $H_{xx} = J/|i-j|^{\alpha}\hat{S}_i^x\hat{S}_j^x$ with discrete $\mathbb{Z}_2$ symmetry. (b) Periodically applying global $\pi/2$ pulses around different axes of the Bloch sphere creates interactions along all three spin directions H_{xx}, H_{yy}, and H_{zz}. (c) The high-frequency limit of such a protocol realizes a long-ranged Heisenberg model H_{LR} with continuous SU(2) symmetry. This model features a quantum phase transition from a dimerized to a liquid phase. Inset: A Binder cumulant analysis of the dimerization determines a critical power-law exponent of $\alpha_c \approx 1.66$.

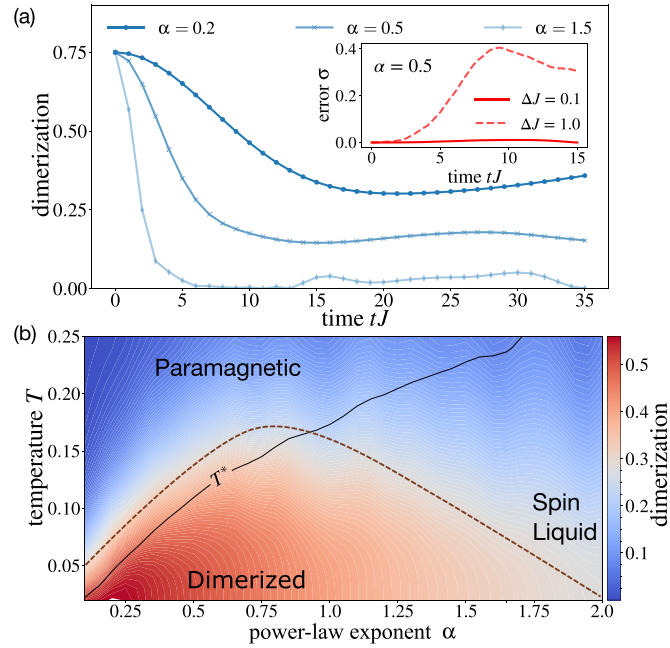

FIG. 2. Dynamical phase diagram. (a) Evolution of the dimerization d under the Floquet dynamics for an initial $|\mathrm{MG}\rangle$ state of singlets. The evolution is governed by $H_{LR}(\alpha)$ for $\alpha \in \{0.2, 0.5, 1.5\}$ and a chain of 64 sites. Inset: We illustrate the relative deviation $\sigma \equiv |(d_{\Delta J\to 0} - d_{\Delta J})/d_{\Delta J\to 0}|$ of the Floquet protocol from the exact evolution for different values of ΔJ and $\alpha = 0.5$. (b) Thermal phase diagram for $H_{LR}(\alpha)$ including the effective temperature T^* of our system (solid line) and a schematic of the phase boundary between the dimerized and the translational invariant phases (dashed dome) for a system of 18 sites.

approximate the power-law coupling by a sum of exponentials [26,27]. An analysis of the Binder cumulant $\langle d^4\rangle/\langle d^2\rangle^2$, that is expected to be scale-independent at criticality [28,29], indicates a quantum phase transition from a dimerized phase to a liquid at $\alpha_c \approx 1.66$ (inset). Precisely extracting the critical point is a formidable challenge, as the transition is in the Berezinskii-Kosterlitz-Thouless universality class [17,30,31]. We emphasize, however, that for the following discussions the precise location of the phase transition is not crucial.

Floquet protocol. Collective vibrations of an ion crystal mediate long-range Ising interactions $H_{xx} = \sum_{i<j} J/|i-j|^{\alpha} S_i^x S_j^x$ [32,33]. Previous works suggested to use multiple phonon branches [34] and quasiperiodic driving [35] to realize Heisenberg type interactions, or have employed digital simulation schemes [36]. Here, instead we suggest periodic driving [37–40] to promote the discrete $\mathbb{Z}_2$ symmetry of the Ising interactions to the continuous SU(2) symmetry of the Heisenberg interactions. The protocol consists of $\pi/2$ pulses around different axes to encircle a surface of the Bloch sphere Fig. 1(b); see Ref. [38] for a related protocol and Refs. [41–43] for recent experimental realizations. The duration δ of the $\pi/2$ pulses can be chosen to be much shorter than the waiting time Δ, leading to an effective period of $\approx 3\Delta$. This way the many-body state rotates periodically from the x over y to z direction. These unitary transformations can also be interpreted to act on the Hamiltonian instead of the many-body state, leading to an effective time evolution with alternating H_{xx}, H_{yy}, and H_{zz} Ising couplings. Provided the rate Δ^{-1} is fast compared to the typical interaction strength J, a high-frequency expansion [44] for the effective periodic drive can be computed, which to leading order yields the SU(2) invariant Hamiltonian Eq. (1).

Singlet evolution. As a direct application of our Floquet protocol, we compute the time evolution of the long-range Heisenberg model $H_{LR}(\alpha)$ for an initial singlet state $|\mathrm{MG}\rangle$ using the time-dependent variational principle for MPS [45–49]. For quenches to small α, we find that the dimerization remains finite at long times, whereas it quickly decays to zero for quenches to large α; see Fig. 2(a). To compare the discrete Floquet evolution with the exact dynamics of $H_{LR}(\alpha)$, we introduce the relative deviation $\sigma \equiv |(d_{\Delta J\to 0} - d_{\Delta J})/d_{\Delta J\to 0}|$, shown in the inset of Fig. 2(a) for $\alpha = 0.5$. We find that the Floquet protocol accurately describes the SU(2) invariant Heisenberg evolution for $\Delta J = 0.1$ (depending on α, larger values of $\Delta J \approx 1$ can be safely reached [21]).

The energy density of the dimerized initial state is $\langle \mathrm{MG}|H_{LR}(\alpha)|\mathrm{MG}\rangle/L = -0.375J$ independent of α, which is larger than the ground-state energy density of $H_{LR}(\alpha)$. Hence, the quench deposits an extensive amount of energy into the system. According to the eigenstate thermalization hypothesis [50–52], which is expected to hold for generic

interacting systems as this, a subsystem should thermalize to an effective temperature T^*, that is consistent with the energy density deposited in the system. The effective temperature can then be evaluated self-consistently from the condition $\langle \mathrm{MG}|H_{\mathrm{LR}}(\alpha)|\mathrm{MG}\rangle = \mathrm{tr}[H_{\mathrm{LR}}(\alpha)e^{-H_{\mathrm{LR}}(\alpha)/T^*}/\mathcal{Z}]$ where $\mathcal{Z}$ is the partition sum. We approximate the thermal expectation value using the typicality approach [53] and evolve 50 random initial states in imaginary time using exact diagonalization on 18 spins (see Ref. [21] for system size dependence) to extract effective temperature T^* as a function of α; Fig. 2(b). From the dynamical phase diagram, we find that for $\alpha \lesssim 1$ the effective temperature is low enough such that a finite dimerization is supported in the steady state, whereas it decays to zero for $\alpha \gtrsim 1$, consistent with our observations on the time evolution in Fig. 2(a). Despite the one-dimensional character of our system, a sharp finite-temperature phase transition can arise in the thermodynamic limit because of the long-range interactions [54].

Measuring the Zak phase. Starting from the $|\mathrm{MG}\rangle$ state, a state close to the ground state of $H_{\mathrm{LR}}(\alpha)$ can be prepared by adiabatically tuning α as long as the system remains in the dimerized phase. We will now present a protocol to measure a topological order parameter of such a state. Following Refs. [55,56], we introduce the SU(2) transformation

$$\Phi : \vec{S}_i \cdot \vec{S}_j \;\mapsto\; \hat{S}_i^z \hat{S}_j^z + \tfrac{1}{2}(e^{i\varphi}\hat{S}_i^+ \hat{S}_j^- + \mathrm{H.c.}), \tag{4}$$

where φ is a compact variable in the interval $[0, 2\pi]$. The SU(2) transformation is designed such that it affects only couplings crossing the ℓth bond between sites ℓ and $\ell+1$, which separates our system into a left S_L and a right S_R part. All interactions within one subsystem remain unchanged. As a consequence we obtain for every choice of the bond ℓ a new family of Hamiltonians $H_{\mathrm{LR}}(\alpha;\varphi)$ parametrized by $\varphi \in [0, 2\pi]$.

A key for obtaining a quantized topological order parameter is that the chosen parametrization retains the time-reversal symmetry of $H_{\mathrm{LR}}(\alpha;\varphi)$ [55]. Tuning φ continuously through the interval $[0, 2\pi]$, describes a closed loop $\mathcal{C}_\ell$ within the set of Hamiltonians. This allows us to introduce the Zak phase

$$\gamma_\ell^{\mathrm{Zak}} = \oint_{\mathcal{C}_\ell} d\varphi \langle \psi(\varphi)|i\partial_\varphi|\psi(\varphi)\rangle, \tag{5}$$

where $|\psi(\varphi)\rangle$ is the ground state of $H_{\mathrm{LR}}(\alpha;\varphi)$. The Zak phase is well defined, provided the corresponding path C_ℓ is followed adiabatically, which can be ensured because the dimerized phase is gapped; see the Supplemental Material [21]. In order to gain some intuition about the Zak phase, we first apply the SU(2) transformation to the fully dimerized $|\mathrm{MG}\rangle$ state. When the bond ℓ lies within a singlet, the transformation gives $(|\uparrow\downarrow\rangle - e^{i\varphi}|\downarrow\uparrow\rangle)/\sqrt{2}$. Evaluating Eq. (5) for this particular case reveals a Zak phase of π [57,58], while it is zero when the bond ℓ lies between two singlets. For the $|\mathrm{MG}\rangle$ state and thus also for the adiabatically connected ordered ground states of H_{LR} we consequently expect to find a Zak phase alternating between values of 0 or π when traversing the bond ℓ through the system.

Before we numerically compute the Zak phase of the dimerized state, we introduce a protocol to experimentally measure it in a trapped ion setting. Let us first gain some intuition: To realize a transformation similarly to (4), we can use an effective (in general time-dependent) magnetic field $B_i^{\mathrm{eff}}(t)$ acting on the spins of $H_{\mathrm{LR}}(\alpha)$, that is proportional to a step function with the step being located at bond ℓ. Using the Peierls substitution, the magnetic field can be absorbed into Hamiltonian as $H_{\mathrm{LR}}(\alpha;\varphi(t)) = \sum_{i<j} J/|i-j|^\alpha [S_i^z S_j^z + \frac{1}{2}(e^{i\varphi_{ij}(t)} S_i^+ S_j^- + \mathrm{H.c.})]$, where $\varphi_{ij}(t) \equiv \int_0^t dt' [B_j^{\mathrm{eff}}(t') - B_i^{\mathrm{eff}}(t')]$. A phase is only picked up, when bond ℓ is crossed as B_i^{eff} is assumed to be constant except across bond ℓ. The time t is chosen such that the phase φ is adiabatically tuned from 0 to 2π. The Zak phase can be measured using a Ramsey sequence to cancel dynamical phases [59–61].

In order to implement this approach in a chain of ions, we identify the leftmost ion as an ancilla qubit τ^z that operates on the same computational basis and has the same power-law coupling to the other spins of the chain $\sum_i J/|i|^\alpha \tau^z \hat{S}_i^z \equiv \sum_i B_i^{\mathrm{eff}} \hat{S}_i^z$. The protocol then consists of the following steps; see Figs. 3(a) and 3(b) for an illustration: (i) After ground-state preparation of the chain initialize the ancilla qubit in a superposition state by applying a $\pi/2$ rotation. This leads to an opposite sign in B^{eff} for the two ancilla states and in turn allows for a cancellation of the dynamical phase. (ii) Perform global $\pi/2$ rotations on the system around different axes, as discussed in Fig. 1(c), to realize the long-range Heisenberg dynamics. During that time perform equally spaced π rotations on the ancilla qubit to cancel the phase accumulation from interaction with the remaining chain. (iii) After a Floquet period, apply a π rotation only on the right part of the system to create a kink in the effective field B_i^{eff} at bond ℓ; see Fig. 3(b). Accumulate phase on the ancilla and apply another π rotation to restore the couplings within the system. Steps (ii) and (iii) are then repeated until φ covers the whole interval $[0, 2\pi]$. (iv) Apply a π pulse to the left part of the system, enabling an inverse rotation to compensate the effect of the protocol on the wave function of the system. (v) Measure the phase of the ancilla, which corresponds to the many-body Zak phase at bond ℓ. For a more detailed description, see the Supplemental Material [21]

We now numerically evaluate the Zak phase Eq. (5). Using DMRG we compute the ground state for 20 discretized steps along $\mathcal{C}_\ell$ for a system of 32 sites and $\alpha = 0.2$, see Fig. 3(d), which confirms that the Zak phase is alternating between 0 and π, a characteristics of a dimerized state. We also confirm the adiabaticity of the computation by calculating the product of projectors into the ground state $\mathcal{P}(\varphi) = |\psi(\varphi)\rangle\langle\psi(\varphi)|$ during each step of the protocol, which attains large values between 0.75 to 1.

In the proposed experimental protocol, the effective magnetic field has the required jump at bond ℓ to introduce the local SU(2) transformation, but also varies slowly across the other bonds. By numerically simulating the protocol of Fig. 3, we find that the phase accumulated on the ancilla has the characteristic bond alternating pattern for dimerized states; see the Supplemental Material [21] for details, where we also analyze the number of required operations.

Topological excitations. In order to characterize the topological excitations of the dimerized phase, we now consider a chain with an odd number of sites. In this case, singlets cannot fully cover the chain, and hence an unpaired spin-1/2 (spinon)

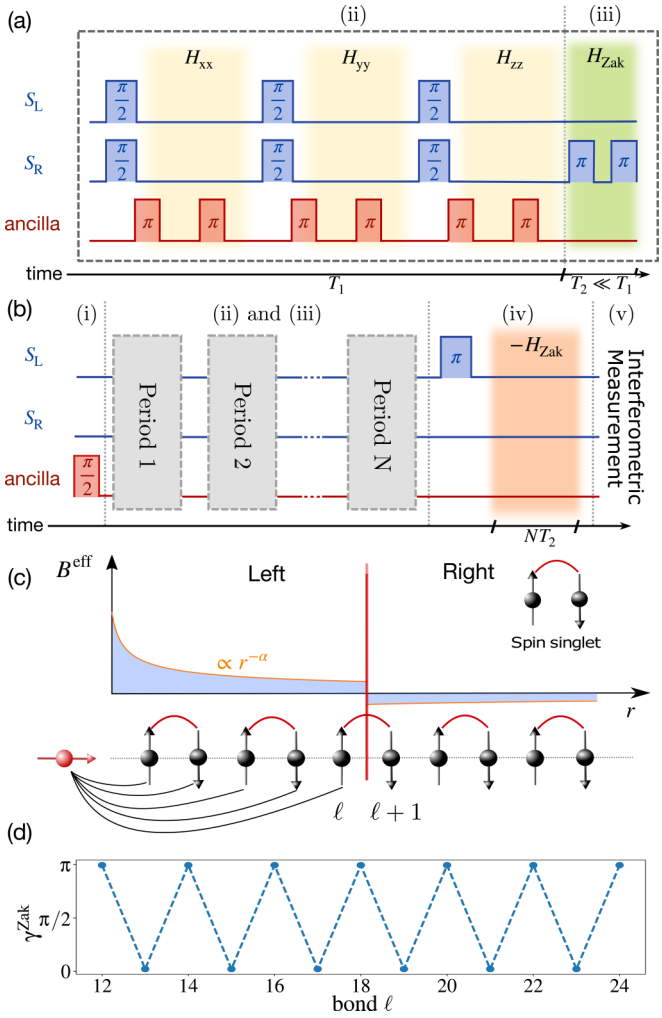

FIG. 3. Measuring many-body Zak phases with interferometry. (a) Single Floquet period and (b) complete pulse sequence for extracting the Zak phase; see main text for details. (c) The effective field B^{eff} acting on the system during the step (iii) of the protocol has a sign change at the bond where we measure γ^{Zak}_ℓ. (d) Performing measurements for different ℓ yields alternating Zak phases of 0 or π. Data are evaluated for a system of 32 sites and $\alpha = 0.2$.

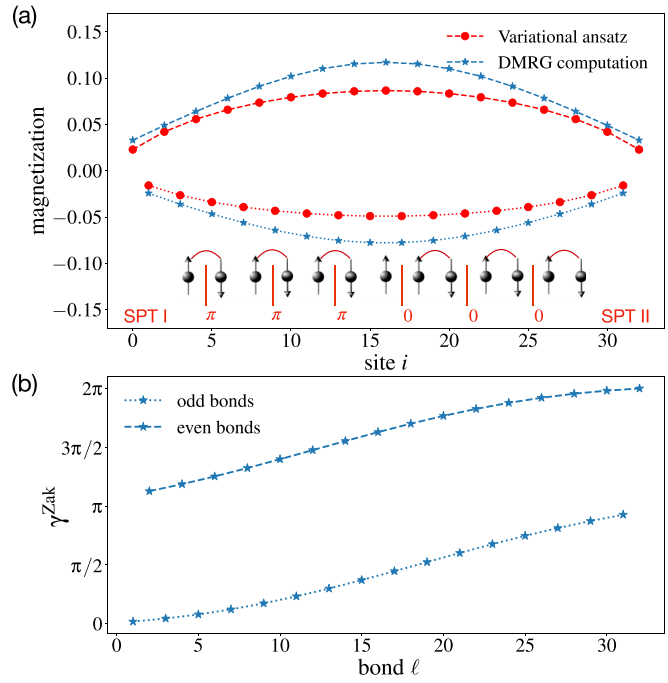

FIG. 4. Topological excitations. (a) Local magnetization for a spinon in a lattice of 33 sites and $\alpha = 0.2$. We compare the DMRG result with a variational ansatz delocalizing a single spinon. (b) This bulk excitation swaps the Zak phase of even and odd bonds as the bond ℓ traverses the system.

excitation is always present. Due to prominent examples such as the Affleck-Kennedy-Lieb-Tasaki (AKLT) model [62], we are used to the existence of spin-1/2 states in interacting topological phases. These degenerate modes provide a clear signature for topological order and are typically localized at the edges of the system. In contrast to the usual edge modes, a measurement of the magnetization for H_{LR} indicates that the excitation is delocalized over the entire lattice; see Fig. 4(a). In order to obtain an analytical understanding, we introduce a variational state that describes a delocalized spinon with wave vector q separating two $|\text{MG}\rangle$ states with singlets on even and odd bonds, respectively [21]. The spinon hence represents a defect in the topological order; see inset of Fig. 4(a). Variationally optimizing the ground-state energy with our ansatz yields $q = \frac{\pi L}{2(L+1)}$, which is consistent with the oscillatory magnetization pattern in Fig. 4(a).

We also characterize the Zak phase for this state. For odd numbers of sites, the dimerized ground state of the system is twofold degenerate due to the SU(2) symmetry of our model and hence we cannot construct an adiabatic path $\mathcal{C}_\ell$. To lift the degeneracy, we apply a weak local magnetic field in the center of the system, which introduces a small gap. This magnetic field breaks time-reversal symmetry. From the arguments of Hatsugai [55,56] it then follows that the Zak phase is not quantized in general. As a consequence, we expect a monotonous change in the Zak phase as we traverse the system which can be interpreted as a mobile domain wall separating two distinct topological phases. This is consistent with our results in Fig. 4(b), which also show that the Zak phase of even and odd bonds differ by π as advocated by the domain wall picture.

Outlook. The Heisenberg model with long-range antiferromagnetic interactions exhibits a phase transition from a liquid to a dimerized valence bond solid that spontaneously breaks the lattice translational invariance. We propose Floquet protocols for trapped ions to realize this model and to characterize the nature of the delocalized topological excitations as well as the bulk topological invariants.

For future studies, it would be interesting to introduce an easy-axis anisotropy by adjusting the Floquet periods between the $\pi/2$ pulses to realize a deconfined quantum critical point between a dimerized and a Néel ordered phase in our one-dimensional model [63,64] or to explicitly break the translational symmetry by introducing bond-alternating couplings to realize a Haldane symmetry protected topological (SPT) phase with localized edge states [18]. A future challenge is to create interacting higher dimensional topologically ordered many-body states with synthetic quantum matter that are characterized by a topological entanglement entropy and fractional excitations [65]. With our protocols, interactions in

two dimensional triangular lattices of trapped ions [66] could be promoted from $\mathbb{Z}_2$ to SU(2) symmetry, with the prospect of realizing exotic frustrated mangetic states or even quantum spin liquids.

Acknowledgements. We thank R. Blatt, E. Demler, Ch. Maier, F. Pollmann, and R. Verresen for insightful discussions. Our tensor-network simulations were performed using the TeNPy Library [48]. We acknowledge support from the Deutsche Forschungsgemeinschaft (DFG, German Research Foundation) under Germany's Excellence Strategy EXC–2111–390814868, TRR80, and DFG Grants No. KN1254/2-1 and No. KN1254/1-2, Research Unit FOR 2414 under Project No. 277974659, and the European Research Council (ERC) under the European Unions Horizon 2020 research and innovation programme (Grant Agreement No. 851161), as well as the Munich Quantum Valley, which is supported by the Bavarian state government with funds from the Hightech Agenda Bayern Plus.

[1] M. Aidelsburger, M. Atala, M. Lohse, J. T. Barreiro, B. Paredes, and I. Bloch, Realization of the Hofstadter Hamiltonian with Ultracold Atoms in Optical Lattices, Phys. Rev. Lett. **111**, 185301 (2013).

[2] H. Miyake, G. A. Siviloglou, C. J. Kennedy, W. C. Burton, and W. Ketterle, Publisher's note: Realizing the Harper Hamiltonian with Laser-Assisted Tunneling in Optical Lattices Phys. Rev. Lett. **111**, 185302 (2013) [**111**, 199903(E) (2013)].

[3] G. Jotzu, M. Messer, R. Desbuquois, M. Lebrat, T. Uehlinger, D. Greif, and T. Esslinger, Experimental realization of the topological haldane model with ultracold fermions, Nature (London) **515**, 237 (2014).

[4] N. Fläschner, B. S. Rem, M. Tarnowski, D. Vogel, D.-S. Luhmann, K. Sengstock, and C. Weitenberg, Experimental reconstruction of the Berry curvature in a Floquet Bloch band, Science **352**, 1091 (2016).

[5] K. Wintersperger, C. Braun, F. N. Ünal, A. Eckardt, M. Di Liberto, N. Goldman, I. Bloch, and M. Aidelsburger, Realization of an anomalous Floquet topological system with ultracold atoms, Nat. Phys. **16**, 1058 (2020).

[6] M. E. Tai, A. Lukin, M. Rispoli, R. Schittko, T. Menke, D. Borgnia, P. M. Preiss, F. Grusdt, A. M. Kaufman, and M. Greiner, Microscopy of the interacting Harper-Hofstadter model in the two-body limit, Nature (London) **546**, 519 (2017).

[7] P. Roushan, C. Neill, A. Megrant, Y. Chen, R. Babbush, R. Barends, B. Campbell, Z. Chen, B. Chiaro, A. Dunsworth, A. Fowler, E. Jeffrey, J. Kelly, E. Lucero, J. Mutus, P. J. J. O'Malley, M. Neeley, C. Quintana, D. Sank, A. Vainsencher *et al.*, Chiral ground-state currents of interacting photons in a synthetic magnetic field, Nat. Phys. **13**, 146 (2017).

[8] Z.-C. Gu and X.-G. Wen, Tensor-entanglement-filtering renormalization approach and symmetry-protected topological order, Phys. Rev. B **80**, 155131 (2009).

[9] F. Pollmann, E. Berg, A. M. Turner, and M. Oshikawa, Symmetry protection of topological phases in one-dimensional quantum spin systems, Phys. Rev. B **85**, 075125 (2012).

[10] S. de Léséleuc, V. Lienhard, P. Scholl, D. Barredo, S. Weber, N. Lang, H. P. Büchler, T. Lahaye, and A. Browaeys, Observation of a symmetry-protected topological phase of interacting bosons with Rydberg atoms, Science **365**, 775 (2019).

[11] P. Sompet, S. Hirthe, D. Bourgund, T. Chalopin, J. Bibo, J. Koepsell, P. Bojović, R. Verresen, F. Pollmann, G. Salomon, C. Gross, T. A. Hilker, and I. Bloch, Realising the symmetry-protected haldane phase in Fermi-Hubbard ladders, arXiv:2103.10421.

[12] K. J. Satzinger, Y. Liu, A. Smith, C. Knapp, M. Newman, C. Jones, Z. Chen, C. Quintana, X. Mi, A. Dunsworth, C. Gidney *et al.*, Realizing topologically ordered states on a quantum processor, Science **374**, 1237 (2021).

[13] G. Semeghini, H. Levine, A. Keesling, S. Ebadi, T. T. Wang, D. Bluvstein, R. Verresen, H. Pichler, M. Kalinowski, R. Samajdar, A. Omran, S. Sachdev, A. Vishwanath, M. Greiner, V. Vuletić, and M. D. Lukin, Probing topological spin liquids on a programmable quantum simulator, Science **374**, 1242 (2021).

[14] R. Blatt and C. F. Roos, Quantum simulations with trapped ions, Nat. Phys. **8**, 277 (2012).

[15] C. K. Majumdar and D. K. Ghosh, On next-nearest-neighbor interaction in linear chain. I, J. Math. Phys. **10**, 1388 (1969).

[16] C. K. Majumdar and D. K. Ghosh, On next-nearest-neighbor interaction in linear chain. II, J. Math. Phys. **10**, 1399 (1969).

[17] S. R. White and I. Affleck, Dimerization and incommensurate spiral spin correlations in the zigzag spin chain: Analogies to the Kondo lattice, Phys. Rev. B **54**, 9862 (1996).

[18] F. D. M. Haldane, Continuum dynamics of the 1-D Heisenberg antiferromagnet: Identification with the O(3) nonlinear sigma model, Phys. Lett. A **93**, 464 (1983).

[19] Z.-X. Gong, M. F. Maghrebi, A. Hu, M. L. Wall, M. Foss-Feig, and A. V. Gorshkov, Topological phases with long-range interactions, Phys. Rev. B **93**, 041102(R) (2016).

[20] T. Giamarchi, *Quantum Physics in One Dimension* (Oxford University Press, Oxford, UK, 2004).

[21] See Supplemental Material at http://link.aps.org/supplemental/10.1103/PhysRevB.105.L241103 for details about representation theory of the SU(2) group and ground state configurations, as well as numerical investigations of Floquet protocols and measurements of Zak phases.

[22] J. F. Cornwell and W. W. Buck, Group theory in physics: An introduction, Phys. Today **51**(9), 67 (1998).

[23] W. Marshall, Antiferromagnetism, Proc. R. Soc. London A **232**, 48 (1955).

[24] F. D. M. Haldane, Nonlinear Field Theory of Large-Spin Heisenberg Antiferromagnets: Semiclassically Quantized Solitons of the One-Dimensional Easy-Axis Néel State, Phys. Rev. Lett. **50**, 1153 (1983).

[25] F. Verstraete, V. Murg, and J. I. Cirac, Matrix product states, projected entangled pair states, and variational renormalization group methods for quantum spin systems, Adv. Phys. **57**, 143 (2008).

[26] U. Schollwoeck, The density-matrix renormalization group in the age of matrix product states, Ann. Phys. **326**, 96 (2011).

[27] B. Pirvu V. Murg, J. I. Cirac, B. Pirvu, and F. Verstraete, Matrix product operator representations, New J. Phys. **12**, 025012 (2010).

[28] K. Binder and D. W. Heermann, *Monte Carlo Simulation in Statistical Physics*, 5th ed. (Springer, Heidelberg, 2010).

[29] D. P. Landau and K. Binder, *A Guide to Monte Carlo Simulations in Statistical Physics*, 4th ed. (Cambridge University Press, Cambridge, UK, 2015).

[30] S. Eggert and I. Affleck, Magnetic impurities in half-integer-spin Heisenberg antiferromagnetic chains, Phys. Rev. B **46**, 10866 (1992).

[31] S. Eggert, Numerical evidence for multiplicative logarithmic corrections from marginal operators, Phys. Rev. B **54**, R9612(R) (1996).

[32] P. Richerme, Z.-X. Gong, A. Lee, C. Senko, J. Smith, M. Foss-Feig, S. Michalakis, A. V. Gorshkov, and C. Monroe, Non-local propagation of correlations in quantum systems with long-range interactions, Nature (London) **511**, 198 (2014).

[33] P. Jurcevic, B. P. Lanyon, P. Hauke, C. Hempel, P. Zoller, R. Blatt, and C. F. Roos, Quasiparticle engineering and entanglement propagation in a quantum many-body system, Nature (London) **511**, 202 (2014).

[34] D. Porras and J. I. Cirac, Effective Quantum Spin Systems with Trapped Ions, Phys. Rev. Lett. **92**, 207901 (2004).

[35] A. Bermudez, L. Tagliacozzo, G. Sierra, and P. Richerme, Long-range Heisenberg models in quasiperiodically driven crystals of trapped ions, Phys. Rev. B **95**, 024431 (2017).

[36] B. P. Lanyon, C. Hempel, D. Nigg, M. Muller, R. Gerritsma, F. Zahringer, P. Schindler, J. T. Barreiro, M. Rambach, G. Kirchmair *et al.*, Universal digital quantum simulation with trapped ions, Science **334**, 57 (2011).

[37] J. Choi, H. Zhou, H. S. Knowles, R. Landig, S. Choi, and M. D. Lukin, Robust Dynamic Hamiltonian Engineering of Many-Body Spin Systems, Phys. Rev. X **10**, 031002 (2020).

[38] I. Arrazola, J. S. Pedernales, L. Lamata, and E. Solano, Digital-analog quantum simulation of spin models in trapped ions, Sci. Rep. **6**, 30534 (2016).

[39] V. Kasper, T. V. Zache, F. Jendrzejewski, M. Lewenstein, and E. Zohar, Non-Abelian gauge invariance from dynamical decoupling, arXiv:2012.08620.

[40] K. Agarwal and I. Martin, Dynamical Enhancement of Symmetries in Many-Body Systems, Phys. Rev. Lett. **125**, 080602 (2019).

[41] S. Geier, N. Thaicharoen, C. Hainaut, T. Franz, A. Salzinger, A. Tebben, D. Grimshandl, G. Zürn, and M. Weidemüller, Floquet Hamiltonian engineering of an isolated many-body spin system, Science **374**, 1149 (2021).

[42] P. Scholl, H. J. Williams, G. Bornet, F. Wallner, D. Barredo, L. Henriet, A. Signoles, C. Hainaut, T. Franz, S. Geier, A. Tebben, A. Salzinger, G. Zrn, T. Lahaye, M. Weidemüller, and A. Browaeys, Microwave-engineering of programmable XXZ Hamiltonians in arrays of Rydberg atoms, PRX Quantum **3**, 020303 (2022).

[43] F. Kranzl, A. Lasek, M. K. Joshi, A. Kalev, R. Blatt, C. F. Roos, and N. Y. Halpern, Experimental observation of thermalisation with noncommuting charges, arXiv:2202.04652.

[44] M. Bukov, L. D'Alessio, and A. Polkovnikov, Universal high-frequency behavior of periodically driven systems: From dynamical stabilization to floquet engineering, Adv. Phys. **64**, 139 (2015).

[45] J. Haegeman, J. I. Cirac, T. J. Osborne, I. Pižorn, H. Verschelde, and F. Verstraete, Time-Dependent Variational Principle for Quantum Lattices, Phys. Rev. Lett. **107**, 070601 (2011).

[46] J. Haegeman, C. Lubich, I. Oseledets, B. Vandereycken, and F. Verstraete, Unifying time evolution and optimization with matrix product states, Phys. Rev. B **94**, 165116 (2016).

[47] B. Žunkovič, M. Heyl, M. Knap, and A. Silva, Dynamical Quantum Phase Transitions in Spin Chains with Long-Range Interactions: Merging Different Concepts of Nonequilibrium Criticality, Phys. Rev. Lett. **120**, 130601 (2018).

[48] J. Hauschild and F. Pollmann, Efficient numerical simulations with Tensor Networks: Tensor Network Python (TeNPy), SciPost Phys. Lect. Notes 5 (2018).

[49] J. C. Halimeh, V. Zauner-Stauber, I. P. McCulloch, I. de Vega, U. Schollwöck, and M. Kastner, Prethermalization and persistent order in the absence of a thermal phase transition, Phys. Rev. B **95**, 024302 (2016).

[50] J. M. Deutsch, Quantum statistical mechanics in a closed system, Phys. Rev. A **43**, 2046 (1991).

[51] M. Srednicki, Chaos and quantum thermalization, Phys. Rev. E **50**, 888 (1994).

[52] M. Rigol, V. Dunjko, and M. Olshanii, Thermalization and its mechanism for generic isolated quantum systems, Nature (London) **452**, 854 (2008).

[53] C. Bartsch and J. Gemmer, Dynamical Typicality of Quantum Expectation Values, Phys. Rev. Lett. **102**, 110403 (2009).

[54] A. Auerbach, *Interacting Electrons and Quantum Magnetism* (Springer, Berlin, 1994).

[55] Y. Hatsugai, Quantized Berry phases for a local characterization of spin liquids in frustrated spin systems, J. Phys.: Condens. Matter **19**, 145209 (2007).

[56] Y. Hatsugai, Quantized Berry phases as local order parameters of quantum liquids, J. Phys. Soc. Jpn. **75**, 123601 (2006).

[57] F. Grusdt, N. Y. Yao, and E. Demler, Topological polarons, quasiparticle invariants, and their detection in 1D symmetry-protected phases, Phys. Rev. B **100**, 075126 (2019).

[58] F. Grusdt, D. Abanin, and E. Demler, Measuring Z2 topological invariants in optical lattices using interferometry, Phys. Rev. A **89**, 043621 (2014).

[59] M. Atala, M. Aidelsburger, J. T. Barreiro, D. Abanin, T. Kitagawa, E. Demler, and I. Bloch, Direct measurement of the Zak phase in topological Bloch bands, Nat. Phys. **9**, 795 (2013).

[60] L. Duca, T. Li, M. Reitter, I. Bloch, M. Schleier-Smith, and U. Schneider, An Aharonov-Bohm interferometer for determining Bloch band topology, Science **347**, 288 (2015).

[61] D. A. Abanin, T. Kitagawa, I. Bloch, and E. Demler, Interferometric Approach to Measuring Band Topology in 2D Optical Lattices, Phys. Rev. Lett. **110**, 165304 (2013).

[62] I. Affleck, T. Kennedy, E. H. Lieb, and H. Tasaki, Rigorous Results on Valence-Bond Ground States in Antiferromagnets, Phys. Rev. Lett. **59**, 799 (1987).

[63] C. Mudry, A. Furusaki, T. Morimoto, and T. Hikihara, Quantum phase transitions beyond Landau-Ginzburg theory in one-dimensional space revisited, Phys. Rev. B **99**, 205153 (2019).

[64] B. Roberts, S. Jiang, and O. I. Motrunich, Deconfined quantum critical point in one dimension, Phys. Rev. B **99**, 165143 (2019).

[65] A. Kitaev and J. Preskill, Topological Entanglement Entropy, Phys. Rev. Lett. **96**, 110404 (2006).

[66] J. G. Bohnet, B. C. Sawyer, J. W. Britton, M. L. Wall, A. M. Rey, M. Foss-Feig, and J. J. Bollinger, Quantum spin dynamics and entanglement generation with hundreds of trapped ions, Science **352**, 1297 (2016).